AD-A276 781

Vibrational Spectroscopy at Metal-Solution Interfaces:

Some Perspectives and Prospects for Electrochemical Surface Science

by

M.J. Weaver, N. Kizhakevariam, X. Jiang, I. Villegas, C. Stuhlmann,

A. Tolia, and X. Gao

Prepared for Publication

in

Journal of Electron Spectroscopy and Related Phenomena

94-07830

Department of Chemistry

Purdue University

West Lafayette, Indiana 47907-1393

DTIC
ELECTE
MAR 10 1994
D
E

February 1994

'94 3 9 074

Vibrational Spectroscopy at Metal-Solution Interfaces:
Some Perspectives and Prospects for Electrochemical Surface Science

M.J. Weaver, N. Kizhakevariam, X. Jiang, I. Villegas, C. Stuhlmann, A. Tolia, and X. Gao

Department of Chemistry, Purdue University,
West Lafayette, Indiana 47907-1393, U.S.A.

Some recent applications of surface vibrational spectroscopies to electrochemical and related interfacial systems are illustrated by means of studies undertaken in the authors' laboratory. The utility of infrared reflection-absorption spectroscopy (IRAS) for linking the structural behavior of adsorbates on ordered metal surfaces in electrochemical and vacuum environments is discussed with reference to a vacuum-based study of CO/D_2O coadsorption on Pt(111). The use of atomic-resolution scanning tunneling microscopy in tandem with in-situ IRAS for electrochemical adlayer structural elucidation is noted. Some virtues of surface-enhanced Raman spectroscopy (SERS) for examining metal-adsorbate vibrations on transition metals in both electrochemical and high-pressure gas-phase systems are also briefly illustrated, specifically for rhodium surface oxidation.

1. INTRODUCTION

The last decade or so has witnessed remarkable advances in both the power and diversity of techniques capable of supplying molecular- and atomic-level structural information for metal-solution (i.e. electrochemical) interfaces. The in-situ approaches now available include methods for extracting spatial structural arrangements, most prominently scanning tunneling microscopy (STM) and grazing incidence X-ray scattering (GIXS), as well as for discerning the molecular state and surface bonding of adsorbed species. The acquisition of primary information regarding the latter, however, remains the domain of vibrational spectroscopies. The first such vibrational technique developed for in-situ electrochemical purposes, originating in the late 1970's, was surface-enhanced Raman spectroscopy (SERS)[1]. Beginning in the early 1980's, and fueled by the emergence of reliable Fourier transform spectrometers, infrared reflection-absorption spectroscopy (IRAS) has become a technique of central importance for the characterization of adsorbates on metal surfaces in electrochemical as well as ultrahigh vacuum (uhv) environments[2,3]. Other vibrational techniques, especially sum-frequency generation (SFG)[4], have

recently been advanced for in-situ electrochemical purposes, although so far IRAS and SERS have constituted the major methods utilized in practice.

Not surprisingly given their markedly different spheres of applicability, the electrochemical applications of IRAS and SERS have tended to follow distinctly different research avenues. The evolution of reliable methods for preparing ordered monocrystalline metal surfaces for in-situ electrochemical purposes has triggered increasingly applications of IRAS for elucidating the vibrational properties of such ordered metal-solution interfaces. When combined with the recent growth of detailed spatial structural information for such systems by means of probe microscopies and X-ray techniques, these developments have crystallized the quest of "in-situ electrochemical surface science". This new research topic addresses molecular-/atomic-level structural issues that overlap increasingly with those pursued in uhv-based surface science[5]. Given that IRAS is applicable to both these types of metal interface, it can provide a centrally important link between the vibrational properties of adsorbates in structurally ordered electrochemical and uhv environments[3,5].

A chief objective of this conference paper is to present examples, taken from recent work in

our laboratory, in order to illustrate how IRAS can contribute to our understanding of adsorbate structure and bonding at ordered metal-solution interfaces, and their relationship to metal-uhv systems. Besides a brief description of in-situ studies, including combined IRAS/STM measurements, we discuss in more detail an example of the utility of IRAS applied in conjunction with "uhv electrochemical modeling" tactics. The latter strategy, pioneered by Sass and coworkers[6], involves synthesizing electrochemical interfaces in uhv by dosing metal surfaces with appropriate molecular and ionizable components so to mimic the so-called charged electrode "double layer".

We also note here some applications of SERS for characterizing in combined fashion adsorption and catalysis at metal-solution and metal-gas interfaces. This vibrational technique has attracted only limited attention of late, especially in fundamental surface science. Although restricted largely to polycrystalline surfaces, SERS can nonetheless be applied to a wide range of surface materials, including transition metals, by depositing them as thin films on gold (or silver) substrates[7]. Major virtues of the SERS technique include its virtual freedom from bulk-phase spectral interferences, the availability of a very wide spectral range with high sensitivity even at low vibrational frequencies, and excellent frequency and temporal resolution. We briefly illustrate here its application to the elucidation of transition-metal surface oxidation.

Although the presentation is necessarily somewhat narrow and constrained, an overall objective is to show how these vibrational methods can be utilized to help bridge the gap in chemical/physical understanding that seemingly persists between the electrochemical and vacuum/gas-phase branches of surface science.

2. UTILIZATION OF IRAS IN UHV ELECTROCHEMICAL MODELING

The recent emergence (starting in 1987-8) of IRAS applied to monocrystalline, chiefly Pt-group transition metal, surfaces in electrochemical environments is providing a substantial amount of intriguing new information concerning the vibrational properties of in-situ electrode-solution interfaces[2,3]. One important new opportunity provided by these measurements is the intercomparison of infrared spectra for simple chemisorbates, archetypically (but not exclusively!) carbon monoxide, in corresponding electrochemical and uhv environments[3]. Such information can supply considerable insight into the additional factors (solvation, double-layer fields, etc.) that can influence adsorbate properties in the former systems. One generally limiting factor, for in-situ IRAS, however, is that it is extremely difficult to avoid completely spectral interferences from the bulk solution, especially the solvent, even when using the conventional experimental tactics which combine thin-layer spectroelectrochemical cells with electrode potential-difference techniques[2].

There is more than one persuasive reason, then, to scrutinize the infrared properties of uhv-based interfaces dosed with one or more of the molecular and ionic components that collectively form the "electrochemical double layer". Such "uhv electrochemical modeling" tactics, already mentioned, can provide a means of assessing the mutual influence of these interfacial components on each other, by examining the spectral and other interfacial properties under sequential dosing conditions. Moreover, the vacuum environment avoids the bulk-phase spectral interferences faced with in-situ methods, and enables a full range of uhv-based techniques to be harnessed, including those applicable also in electrochemical environments.

Although vibrational spectroscopy has formed an integral part of uhv electrochemical modeling studies undertaken to date, electron energy loss spectroscopy (EELS) has been employed almost exclusively[8]. While EELS offers some advantages, the utilization of IRAS for this purpose is clearly of substantial interest, partly to facilitate comparison with in-situ electrochemical spectral data. We now outline a study along these lines for the coadsorption of carbon monoxide and water on Pt(111), recently undertaken in our laboratory[9], that illustrates some of the virtues of this approach for unraveling combined solvation and surface field effects on adsorbate bonding. This system was selected not only in view of its archetypical standing
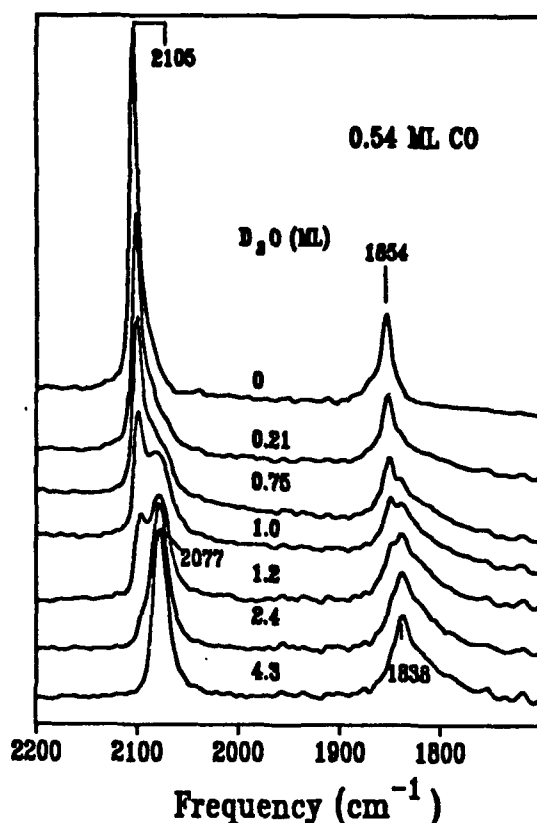
Figure 1. Infrared absorbance spectra in the C-O stretching region for the D_2O coverages indicated with 0.54 monolayers (ML) of predosed CO on Pt(111) in uhv at 100 K.
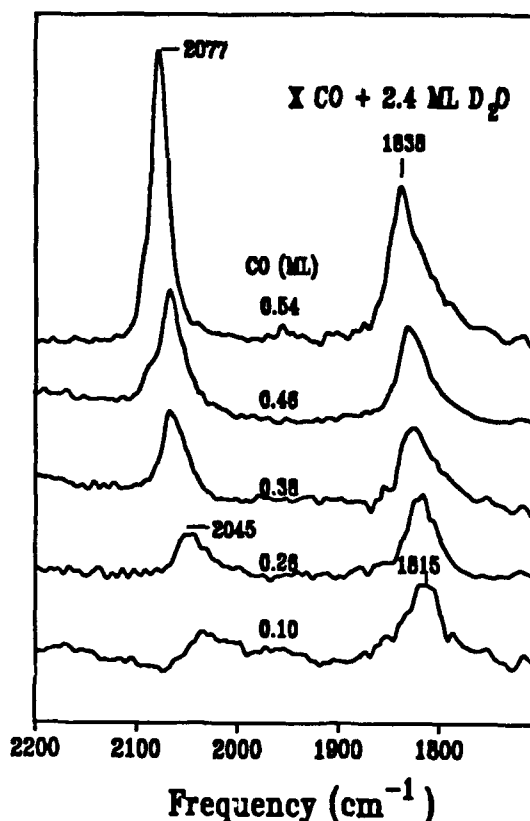

Figure 2. Infrared absorbance spectra in the C-O stretching region for the CO coverages indicated along with 2.4 ML of postdosed D_2O on Pt(111) in uhv at 100 K.

in surface science, but also because of the availability of extensive in-situ electrochemical infrared data for this and related systems[3].

Figure 1 shows infrared spectra in the 1700-2200 cm^{-1} frequency region for a near-saturated coverage ($\theta_{CO} = 0.54$) of CO on Pt(111) at 100 K postdosed with the sequence of increasing D_2O coverages as indicated. (The latter quantities, θ_w, are ratioed to the saturated ice-like "bilayer"[10], which has a coverage of 2/3 relative to the surface metal atoms.) The top spectrum in Fig. 1 displays the characteristic pair of C-O stretching (ν_{CO}) features at 2105 and 1854 cm^{-1}, associated with terminal and twofold-bridging CO, respectively[11,12]. Sequential addition of D_2O is

seen to yield a progressive attenuation of the 2105 cm^{-1} band and a concomitant development of a broader feature at 2077 cm^{-1}. The 1854 cm^{-1} band is also seen to be similarly replaced by a feature peaked at 1838 cm^{-1} under these conditions. These spectral substitutions are virtually complete upon the addition of about 2.5 ML of D_2O. Similar experiments performed at a series of lower CO coverages, down to $\theta_{CO} \sim 0.1$, indicate a increasingly marked change in CO binding from the atop geometry favored exclusively for $\theta_{CO} \leq 1/3$ on clean Pt(111) to a largely bridging coordination.

Infrared spectra for a series of predosed CO coverages as indicated with a fixed large postdosed D_2O coverage ($\theta_w = 2.4$) are shown in Figure 2.
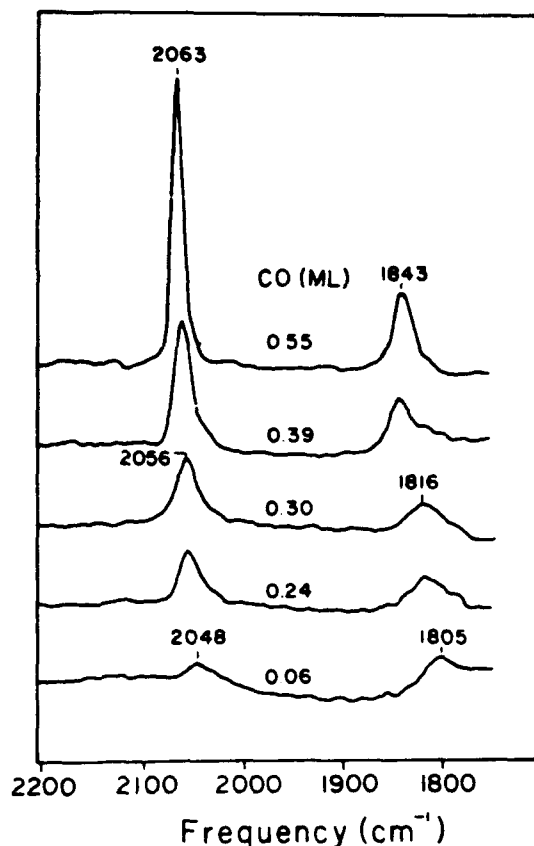
Figure 3. Infrared absorbance spectra in the C-O stretching region for the CO coverages indicated on Pt(111) in aqueous 0.1 M HClO4 at an electrode potential of 0.35 V vs NHE (from ref. 13).

These spectra clearly differ markedly from those obtained in the absence of D2O, and increasingly so towards lower θ_{CO}. Furthermore, the spectra in Fig. 2 bear a close resemblance to those for the analogous electrochemical system. As an illustration of the latter, Fig. 3 shows such a data set for the series of CO coverages indicated on Pt(111) in aqueous 0.1 M HClO4 at 0.35 V vs NHE (normal hydrogen electrode), culled from ref. 13. The similarities between Figs. 2 and 3 with regard both to the θ_{CO}-dependent band frequencies and relative binding-site occupancies, the latter as gleaned from the band intensities, are clearly evident.

Related observations regarding the effect of

coadsorbed water on the vibrational properties of CO on ordered Pt-group surfaces in uhv have been reported previously[14-16]. At least in the context of electrochemical modeling, however, these studies are incomplete in several respects. Perhaps most centrally, in order to establish quantitative links between the infrared spectral behavior of such "solvent coadsorbate" systems in uhv and in-situ electrochemical interfaces it is necessary to have information on the adsorbate-dependent surface potentials present in the former systems, enabling the corresponding spectral data to be compared on a common potential scale[3]. Even though such data are readily obtainable by Kelvin probe or other work-function measurements, they are conspicuous by their absence for CO/water coadsorption. We describe elsewhere such data for the Pt(111)/CO, D2O uhv system[9]; the pertinent findings are now briefly noted.

It is well known that water adsorption on clean Pt(111)[17,18], as on other noble metal surfaces, yields large (ca 1 eV) decreases in work function ascribable both to adsorbate-metal charge transfer and dipole orientation effects[19]. As a consequence, the surface potential ϕ on water-dosed Pt(111) is diminished to values, ca 4.5-5 V, well below that for the clean surface, ca 5.9 V, and comparable to the accessible potentials for CO adsorbed in aqueous electrochemical environments[20]. {Note that the NHE has a potential of about 4.5-4.8 V on the vacuum scale[3], and CO electrooxidation in aqueous acidic electrolytes typically proceed above 0.5-0.6 V vs NHE.} Perhaps surprisingly, the presence of low or moderate CO coverages on Pt(111) yields slightly larger ϕ decreases upon water adsorption, $\Delta\phi$, than on the clean surface, even though $\Delta\phi$ is smaller (about -0.4 V) in the presence of a saturated CO adlayer[9].

A consequence of such $\Delta\phi$ data is that the surface potential for the Pt(111)/CO, D2O system will necessarily vary markedly (by ca 0.7 V) and in nonmonotonic fashion as the CO coverage is altered at high water exposures, as in Fig. 2. Effectively, then, the so-called electrochemical potential of zero charge (ϕ_{pzc}), referring to the absence of net ionic or electronic charges at the interface as mimicked by the Pt(111)/CO, D2O uhv system, undergoes large variations with CO coverage. {Note that a more

"complete" double-layer uhv model would entail the addition of suitable ionizable species such as alkali metals, along with the solvent, allowing ϕ to be adjusted below (or above) ϕ_{pzc}.} By contrast, the infrared data shown for the matching Pt(111)/CO *electrochemical* system in Fig. 3 refers to a *fixed* surface potential, 0.35 V vs NHE (= ca 5.0 V vs vacuum). In the latter case, then, one anticipates that the surface electronic charge, while uniformly negative (i.e. $\phi < \phi_{pzc}$) for the electrochemical system, will vary significantly with CO coverage.

While the validity of the last assertion depends inevitably on the quantitative relevance of the Pt(111)/CO,D_2O uhv system (at 100 K) to the electrochemical system (at 300 K), it is nonetheless clear that the quantitative intercomparison of infrared spectral data between such systems requires receipt of surface potential data for the partner uhv interface. Fortunately, the dependence of the infrared spectral properties for the electrochemical interface upon the surface potential can readily be examined[3,20,21], enabling the ν_{CO} spectra to be compared with those for related uhv interfaces at the same potentials. Undertaking this exercise in the present case (to be detailed elsewhere[9]) indeed yields approximate agreement between the ν_{CO} frequencies and relative terminal/bridging site occupancies as exemplified in Figs. 2 and 3. By this yardstick, then, one has some (albeit incomplete) justification for asserting that the effects of codosing the aqueous solvent along with the adsorbate of interest, carbon monoxide, on Pt(111) alters the surface bonding properties of the latter in a manner which is at least comfortingly similar to those observed for the actual in-situ electrochemical interface.

Such findings encourage further the utilization of infrared spectra for the interfacial solvent, readily obtained for the "electrochemical model" uhv system but essentially unobservable for the in-situ electrochemical system, to shed light on the solvation factors responsible in a manner which is (hopefully) relevant to both types of interfaces. An example of infrared data along these lines is given in Fig. 4, specifically in the O-D stretching region (2150-2800 cm^{-1}) for the increasing CO coverages on Pt(111) in uhv, as indicated, for a fixed D_2O dosage, $\theta_w = 0.75$. In the absence of CO (bottom trace), a broad asymmetric band is observed
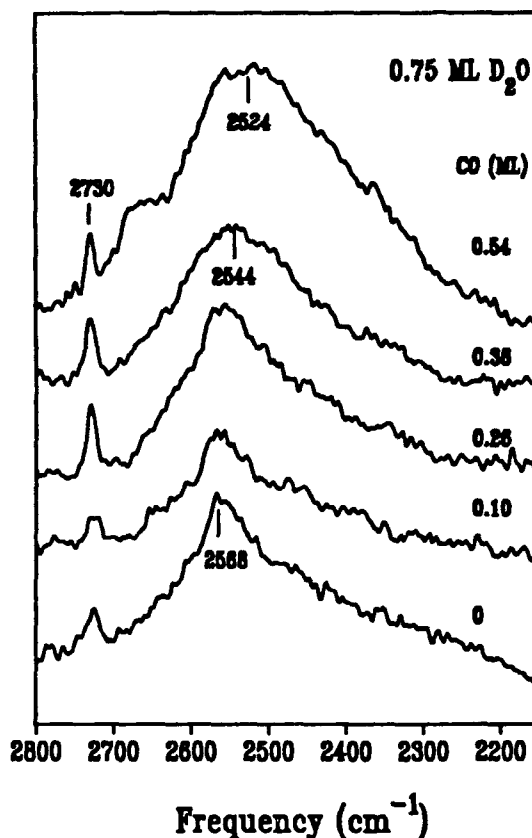

Figure 4. Infrared absorbance spectra in the water O-D stretching region for 0.75 ML D_2O postdosed onto the CO coverages indicated on Pt(111) in uhv at 100 K.

with a peak at 2570 cm^{-1}. Similarly to an earlier infrared study of D_2O on Pt(111)[22], this feature can be ascribed to adsorbed water present in the form of small clusters. The integrated intensity of this band, A_i, on clean Pt(111) shows a nonlinear dependence on water dosage, the A_i-θ_w slope increasing markedly (by ca 4-5 fold) for $\theta_w > 1$, with the band envelope shifting to lower frequencies[9,22]. Since it is well known that increased hydrogen bonding yields markedly larger band intensities as well as significant frequency downshifts[23], this behavior is consistent with the formation of an ice-like bilayer for $\theta_w \geq 1$. The sharp band seen at 2730 cm^{-1} has also been observed previously for adsorbed water layers[10b,24], and is

ascribed here to the stretching vibration of "free" (i.e. not hydrogen-bonded) O-D; in the usual bilayer model 1/4 of the hydrogens are present in this state.

The presence of increasing CO coverages for $\theta_w = 0.75$ is seen to yield a decrease in A_t (for $\theta_{CO} = 0.1$), and then progressive A_t enhancements towards higher θ_{CO} (Fig. 4). This nonmonotonic behavior suggests that at lower CO coverages the small water clusters are dissipated by the need to solvate individual CO molecules. Such solvation in turn can also account for the unexpectedly pronounced work-function decreases seen upon water adsorption under these conditions (vide supra), as well as the atop-bridging CO site conversion engendered by water adsorption. Thus the additional $d\pi$-$2\pi^*$ back bonding characteristic of bridge-bound CO should encourage nearby water molecules to acquire configurations with the polar O-D bond more normal to the surface than in the hydrogen-bound "bilayer" arrangement. Qualitatively similar observations and interpretation have been presented recently for CO and water coadsorbed on Ni(100)[25]. At higher CO coverages on Pt(111), approaching the saturation value $\theta_{CO} \sim 0.65$, there will be insufficient space for the coadsorbed water to contact the surface directly, yielding instead the formation of a hydrogen-bound water film *on top* of the CO adlayer.

This latter circumstance can nonetheless yield significant changes in CO surface bonding, if perhaps less dramatic than caused by "side-by-side" CO/D$_2$O coadsorption, as encountered in Fig. 1. The form of the ν_{CO} spectra in Fig. 1, with a pair of discrete new bands growing in as θ_w is increased, indicates further that water clusters are formed which spread to encompass the entire surface by $\theta_w \sim 2.5$. The ν_{CO} frequency downshift observed under these conditions can largely be understood in terms of electrostatic-field effects induced by the water overlayer[21](cf ref [26]).

The results summarized above are largely consistent with those reported by Wagner et al from an earlier detailed study of CO/D$_2$O coadsorption on Rh(111) and Pt(111) using EELS[15]. These authors concluded, however, that while the Rh(111)/CO,D$_2$O system exhibits the hallmarks of "hydrophilic" coadsorption, involving an intermixed CO/D$_2$O adlayer, the corresponding Pt(111) system involves "hydrophobic" coadsorption, with spatially segregated CO and D$_2$O islands. Nonetheless, the IRAS results noted here (and detailed in ref. 9) show that at lower θ_w the coadsorbed D$_2$O intermixes at least partly with the CO adlayer, rather than merely compressing the latter into separate islands[9].

Overall, there is good reason to be optimistic that IRAS can contribute substantially to the development of a detailed molecular-level understanding of double-layer effects upon adsorbate structure and bonding. The combined and interrelated use of IRAS in uhv and in-situ electrochemical environments constitutes a research tactic that clearly offers multidimensional benefits in this regard.

3. ADLAYER STRUCTURE ELUCIDATION WITH STM/IRAS

An important objective in electrochemical surface science, as for uhv-based systems, is the elucidation of the real-space structure and bonding within ordered adlayers on metal surfaces. The most commonly utilized approach for this purpose in uhv surface science, low-energy electron diffraction (LEED), is essentially inapplicable to in-situ electrochemical interfaces, although much useful information concerning adlayers has been obtained using LEED by transferring electrodes into vacuum[27]. As already mentioned, the recent emergence of STM and GIXS is now enabling such spatial structural information to be obtained for in-situ electrochemical interfaces under potential control. At least for simple molecular adsorbates, the insight into binding geometry and intermolecular interactions that is discernable from vibrational spectroscopy can provide a valuable complement to such spatial structural data. Combined LEED/vibrational spectral measurements have indeed proven useful in analyzing ordered metal-adlayer systems in uhv[28]. One can therefore envisage parallel combinations of STM (or GIXS) with IRAS as a means of discerning electrochemical adlayer structures at a comparable level of depth and detail.

We have recently examined saturated CO adlayers on Rh(111) and (110) by combining in-situ atomic-resolution STM with IRAS data[29,30]. The former system is of particular interest since the infrared spectra show that the CO adlayer undergoes

a potential-induced phase transition, with a preponderance of terminal and bridging CO present on Rh(111) above and below about 0.1 V vs NHE, respectively, in aqueous solution[29]. Markedly different STM images were obtained for these two adlayer phases, having the adlattice symmetries (2 × 2)-3CO and (3 × √3 rect)-4CO, respectively. Comparison with the IRAS data not only supported the validity of the STM images, but also enabled the extraction of reasonably firm assignments of the CO binding sites by comparing the STM intensity patterns with relative site occupancies as gleaned from the IRAS band intensities[29].

The successful utilization of this tactic is clearly limited by several factors, including the need for a sufficiently immobile adlayer to yield stable atomic- (or molecular-) resolution STM images, and the occurrence of an adsorbate vibrational mode which is suitably sensitive to the bonding environment. Carbon monoxide is obviously an excellent candidate from the IRAS perspective. Besides the rhodium examples mentioned above, the Pt(111)/CO system yields suitably stable STM images[31-33].

An additional major virtue of the STM technique is the information afforded concerning nanoscale surface morphology and longer-range as well as local ordering. A good example is provided by the Pt(100)/CO system. Adsorption of CO, more specifically the replacement of adsorbed iodine by CO in aqueous media, is seen to yield dense arrays of small, ca 20-50 Å, substrate islands or mesas[34,35]. While both the mesas and the surrounding lower terraces exhibit (1 × 1) ordered structures, the adsorbate evidently destroys the long-range substrate order seen prior to CO adsorption[35]. Qualitatively similar findings have been obtained for the adsorption of cyanide and sulfide on Pt(100)[35]. Such surface disordering can account for the multiplicity of infrared bands observed, for example for CO on Pt(100), arising from binding at terrace edges as distinct from uniform terrace regions[34,35].

Another example of the use of the combined STM/IRAS approach for the elucidation of adlayer structure studied recently in our laboratory is cyanide on Pt(111)[36]. The upper trace in Fig. 5 is a typical potential-difference infrared (PDIR) spectrum obtained for a saturated adlayer of cyanide
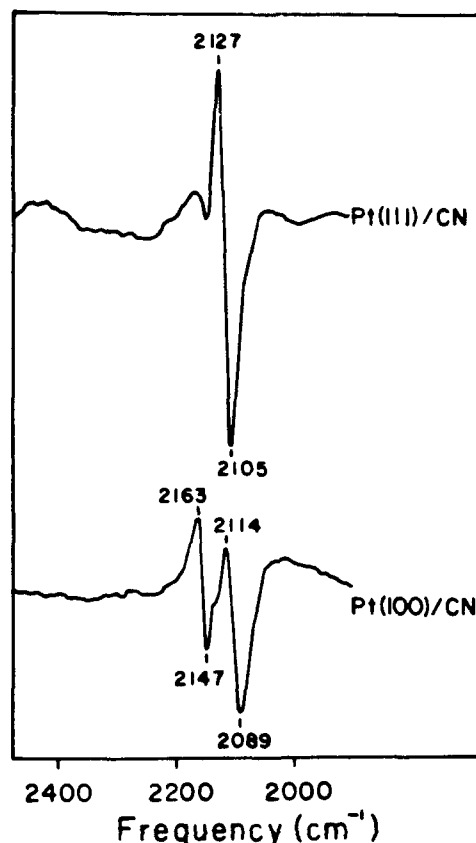

Figure 5. Potential-difference infrared absorbance spectra in C-N stretching region for cyanide adlayers on Pt(111) and Pt(100) as indicated in aqueous 0.1 $\underline{M}$ NaClO$_4$ (pH 10.5). (See text for further details.)

on Pt(111), and the lower trace for Pt(100). Following previous procedures[37,38], the adlayer was formed by immersion of clean Pt(111) or Pt(100) into 1 m$\underline{M}$ NaCN for 3 min at 0.35 V vs NHE, and then transferred to the infrared cell containing 0.1 $\underline{M}$ NaClO$_4$ at pH 10.5. As usual, the bipolar form of the spectra in Fig. 5 results from the presence of adsorbed cyanide at both the "reference" and "sample" potentials, -0.15 and 0.35 V vs NHE, with a significant potential- (or field-) induced band frequency shift. While the Pt(111)/CN⁻ adlayer shows only a single bipolar band, the Pt(100)/CN⁻ system exhibits a pair of bands consistent with more than one form of CN⁻ as would be engendered by
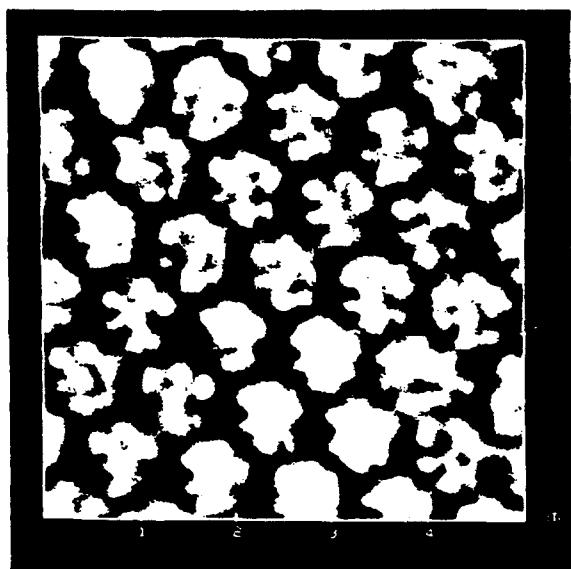
Figure 6. STM image of the $(2\sqrt{3} \times 2\sqrt{3})R30°$ cyanide adlayer on Pt(111) in aqueous 0.1 $\underline{M}$ NaClO$_4$ (pH 10.5) at -0.15 V vs NHE. Adlayer formed using same procedure as in Figure 5 (see text).

two distinct binding environments.

Figure 6 shows a typical STM image for the cyanide adlayer on Pt(111) in 0.1 $\underline{M}$ NaClO$_4$ at about -0.1 V vs NHE. This shows a hexagonal array of patches, each consisting of a central spot surrounded by six nearest neighbors. The rows of hexagonal patches are oriented along the $\sqrt{3}(R30°)$ direction with respect to the Pt substrate rows (as discerned from the x-y crystal orientation). Assuming that each spot corresponds to a single CN, the adlayer structure is deduced to have $(2\sqrt{3} \times 2\sqrt{3})$ symmetry ($\theta_{CN} = 0.58$), in agreement with an earlier ex-situ LEED study[37]. Further details concerning the complete real-space structure, however, can be discerned from the STM image together with the likelihood that essentially a single CN binding site is present, as deduced from the IRAS spectra (Fig. 5). Thus placing the central CN in each "hexagonal patch" in a symmetrical atop site obliges the surrounding six CN's to lie in near-atop sites. Such an arrangement is most consistent with the combined STM/IRAS data, although further work is needed to confirm this possibility.

4. APPLICATION OF SERS TO SURFACE OXIDATION IN ELECTROCHEMICAL AND HIGH-PRESSURE GAS-PHASE SYSTEMS

While most attention in this brief overview is directed towards structural applications of infrared spectroscopy, as noted above SERS offers several attributes which also make it a valuable vibrational technique for some applications[1]. In our own laboratory, SERS is enjoying renewed consideration for the examination of adsorption on metals both in electrochemical and gas-phase environments, especially for reactive systems (e.g. [39-41]). This revival was spawned partly by the extension of the technique to transition metals by electrodeposition as thin films on gold[7], and by the evolution of charge-coupled device (CCD) detector technology[42]. The latter development enables Raman spectra to be acquired with extremely high sensitivity even for the red spectral region in which the SERS effect is observable on gold substrates. As a consequence, one can readily acquire real-time sequences of surface vibrational spectra within ca 1-5 s over wide frequency ranges with essentially complete freedom from the bulk-phase interferences that can plague in-situ IRAS.

We restrict our attention to a brief description of the application of SERS for elucidating surface oxidation processes in aqueous electrochemical and gas-phase systems. This example illustrates the usefulness of SERS for examining surface-adsorbate vibrations (in an analogous fashion to EELS), as well as for establishing further links between metal surface chemistry in electrochemical and gas-phase environments.

It is well known that the electrochemical oxidation of noble-metal, including Pt-group, surfaces is induced in aqueous media by suitable positive alterations in the electrode potential. The oxide so produced can subsequently be reductively removed by lowering the potential. Although there are extensive studies of this surface oxide formation and removal, especially by cyclic voltammetry[43], the microscopic nature and even composition of the films remains ill-understood. Figure 7 shows selected members of a sequence of SER spectra (culled from [41]) obtained for a thin (3-4
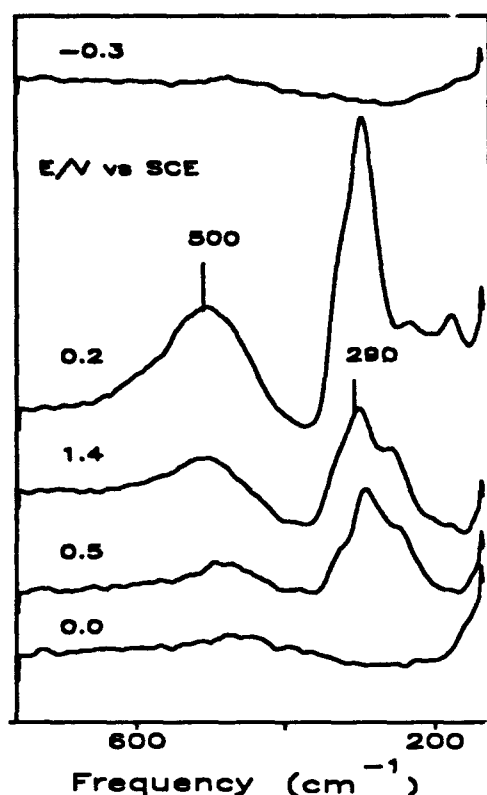
Figure 7. Selected members of SER spectral sequence in metal-oxygen vibrational region for rhodium film on gold in aqueous 0.1 $\underline{M}$ HClO$_4$ during cyclic voltammogram at indicated electrode potentials, showing formation and removal of rhodium oxide (see text for detail; from ref. 41).

monolayer) rhodium film on gold in 0.1 $\underline{M}$ HClO$_4$ during a 10 mV s^{-1} cyclic voltammogram from -0.3 to 1.4 V vs saturated calomel electrode (SCE) and return. (Note that the SCE has a potential of about 0.25 V higher than the NHE.) Each spectrum was acquired over 8 s in the ascending order shown; the electrode potentials indicated refer to the values at the start of each spectral acquisition.

Commencing close to the potential where oxide formation is detected voltammetrically, a pair of Raman bands are observed, consisting of a sharp feature at 290 cm^{-1} and a broader band centered at about 500 cm^{-1}. Both these bands grow in concert as the potential remains at positive values, becoming

especially intense just before (and during) the voltammetric oxide reduction at 0.2-0.3 V, and then disappearing. On the basis of their correlation with the voltammetric behavior (observed simultaneously), these bands can confidently be assigned to rhodium-oxygen vibrations[41]. A broad band at 550-600 cm^{-1} also appears under similar conditions on unmodified gold, but only at higher potentials (> 1.0 V vs SCE). Comparison of the Rh-O spectral features with those for bulk-phase metal oxides indicates that the 290 cm^{-1} band can be assigned to a Rh-O bending vibration, δ_{RhO}, with the ca 500 cm^{-1} feature being associated with a Rh-O stretching vibration arising from a rhodium oxide, probably Rh$_2$O$_3$[41]. The assignment of both these vibrations to Rh-O rather than Rh-OH modes was supported by the absence of a deuterium isotope frequency shift. The 290 and ca 500 cm^{-1} features apparently arise from at least partly distinct surface species. This is evidenced by the selective elimination of the 290 cm^{-1} band in the presence of carbon monoxide[44]. This observation also suggests that the 290 cm^{-1} oxygen species is involved in the catalytic electrooxidation of CO.

Related, yet quite distinct, spectral behavior is observed for the oxidation of other transition metals, specifically platinum and ruthenium[41]. Generally speaking, the tendency to form oxides rather than hydroxides (as deduced from deuterium isotope shift data) increases in the sequence Pt < Au < Rh < Ru, and to a greater extent in acidic compared with alkaline aqueous media. While a single "oxide" species is observed during at least the initial stages of oxidation on the more noble-metal surfaces, ruthenium exhibited more complex behavior, with at least two different Ru oxidation states being discerned from the Raman band frequencies.

One issue of general fundamental interest concerns the relationships between *potential*-induced oxidation observed in aqueous electrochemical systems and the *thermal*-induced oxidation that occurs with O$_2$ (or other O-containing molecules) for metals in the gas phase. The SERS technique enables this issue to be addressed in a relatively direct fashion. As a simple illustrative example, Fig. 8 shows a set of SER spectra obtained for the temperature-programmed oxidation of a similar rhodium film surface as in Fig. 7, but in a gas-phase
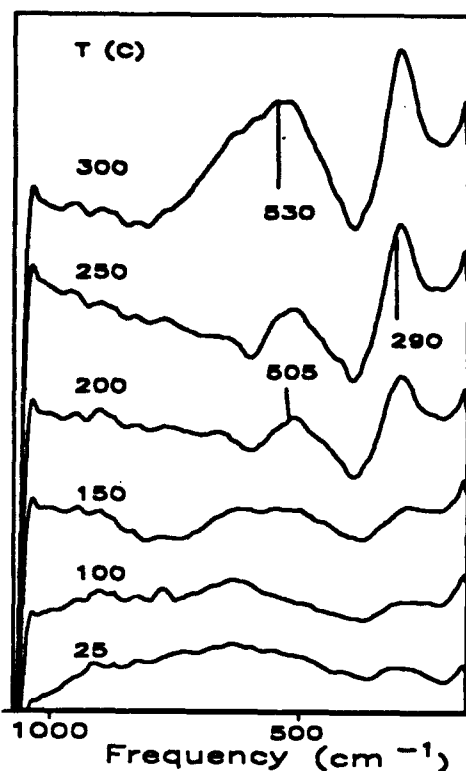
Figure 8. SER spectra for thermal oxidation of rhodium film on gold in atmospheric pressure of 30% O$_2$ and 70% Ar, at ascending temperatures as indicated (see text).

of the gas-phase system is that further analysis of the oxide formed can readily be performed by means of X-ray photoelectron spectroscopy (XPS), albeit after pumping down to reach uhv conditions. These separate experiments strongly support the presence of an oxide species of stoichiometry Rh$_2$O$_3$[45].

Related similarities are also seen by means of SERS for the electrochemical and gas-phase oxidation of ruthenium[45]. Extensions of such parallel electrochemical and gas-phase surface oxidation studies to a number of other metal surfaces are clearly tractable, as are the examination of other interfacial processes, such as the catalytic oxidation of a variety of inorganic or organic species[39].

Finally, in considering such applications of vibrational spectroscopy to surface oxide formation, it is appropriate to mention a complementary application of in-situ STM in this regard. Figure 9 shows a nanoscale STM image of a Au(111) surface in contact with 0.1 M HClO$_4$. During the data acquisition, involving the tip being rastered from the top to bottom of the image as shown, the potential is swept from about 1.25 V to 1.0 V vs NHE, so to
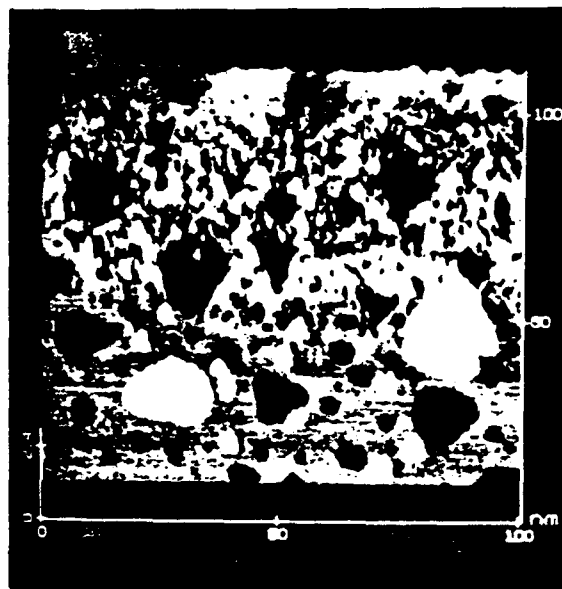
environment consisting of 30% O$_2$ and 70% Ar, at one atmosphere total pressure. The spectra were obtained again in ascending order, spending about 2 min at each temperature shown. A detailed description will be available elsewhere[45].

Briefly, there is an interesting similarity in the form of the spectra for E- and T- induced rhodium surface oxidation in Figs. 7 and 8, respectively. The gas-phase SERS data also support the assignment of the 290 and 500 cm^{-1} bands to distinct oxygen species. Thus for more extensive surface oxidation as induced by stepping the temperature immediately to high values (> 200°C), the 290 cm^{-1} band only appears as a transient intermediate, giving way to almost exclusive formation of the 500 cm^{-1} feature[45]. An advantage

Figure 9. STM image of Au(111) in aqueous 0.1 M HClO$_4$ obtained during potential-induced reduction of oxide film. Potential swept at 15 mV s^{-1} from 1.25 V (top) to 1.0 V vs NHE (bottom) during image acquisition (see text).

reduce voltammetrically the gold oxide that was formed anodically immediately beforehand. As a consequence, the y-axis can be considered as a linear scale of electrode potential (and time), as well as the real-space dimensions as labelled. Interestingly, as ι е oxide starts to reduce (as discerned simultaneously by voltammetry), the surface exhibits marked atomic-scale roughness, these undulations nonetheless disappearing (towards the bottom of the image) as the oxide reduction nears completion. Details will be available elsewhere[46].

The significance of this finding in the present context is the place-exchange process associated with the formation and removal of metal oxide can lead at least transiently to significant changes in the surface morphology. Indeed, such nanoscale roughness can account for the common observation of unusually intense metal-oxygen vibrational bands *during* the reduction of the oxide films[41], given that the SERS effect is intimately associated with the presence of surface undulations. More generally, this example points again to the complementary utility of surface vibrational techniques, which necessarily probe local bonding, with scanning probe microscopies that can yield atomic- or nanoscale-level information on surface structure and morphology.

Overall, then, there are good reasons to be optimistic that vibrational spectroscopies will contribute on an increasingly broad front to the development of a true atomic- and molecular-level understanding of interfacial electrochemical systems. A number of significant topics have not been addressed here, such as the application of both IRAS and SERS in real-time fashion to the examination of molecular electrochemical processes. Indeed, the increasing breadth as well as depth of such vibrational spectroscopic applications in surface electrochemistry is an encouraging sign. Perhaps most importantly, however, such research directions offer real promise that the time-honored gulf between electrochemical and vacuum-based metal interfacial systems is finally giving way to the development of a truly common atomic-/molecular-level understanding in these distinct yet fundamentally allied branches of surface science.

ACKNOWLEDGMENTS

REFERENCES

[1] For a recent review, see: B. Pettinger, in "Adsorption of Molecules at Metal Electrodes", Frontiers of Electrochemistry, Vol. 1, J. Lipkowski, P.N. Ross, eds., VCH Publishers, 1992, Chapter 6.

[2] For a recent review, see: R.J. Nichols in ref. 1, Chapter 7.

[3] S-C. Chang and M.J. Weaver, J. Phys. Chem., 95 (1991), 5391, and references quoted therein.

[4] P. Guyot-Sionnest and A. Tadjeddine, Chem. Phys. Lett., 172 (1990), 341.

[5] M.J. Weaver and X. Gao, Ann. Rev. Phys. Chem., 44 (1993), in press.

[6] For example: J.K. Sass and K. Bange, ACS Symp. Ser. 378 (1988), 54.

[7] L-H.W. Leung and M.J. Weaver, J. Am. Chem. Soc., 109 (1987), 5113.

[8] For a recent review, see F.T. Wagner, in Frontiers of Electrochemistry, Vol. 2, J. Lipkowski, P.N. Ross, eds., VCH publishers, 1993.

[9] N. Kizhakevariam, X. Jiang, and M.J. Weaver, to be submitted to J. Chem. Phys.

[10] (a) D.L. Doering and T.E. Madey, Surf. Sci., 123 (1983), 305; (b) F.T. Wagner and T.E. Moylan, Surf. Sci., 191 (1987), 121.

[11] M. Tüshaus, E. Schweizer, P. Hollins, and A.M. Bradshaw, J. Electron. Spect. Related Phenom., 44 (1987), 305, and previous references cited therein.

[12] E. Schweizer, B.N.J. Persson, M. Tüshaus, D. Hoge, and A.M. Bradshaw, Surf. Sci., 213 (1989), 49.

[13] S-C. Chang and M.J. Weaver, J. Chem. Phys., 92 (1990), 4582.

[14] W.J. Tornquist and G.L. Griffin, J. Vac. Sci. Tech., A4 (1986), 1437.

[15] F.T. Wagner, T.E. Moylan, and S.J. Schmieg, Surf. Sci., 195 (1988), 403.

[16] L-W.H. Leung and D.W. Goodman, Langmuir, 7 (1991), 493.

[17] G.B. Fisher, GMR-4007, General Motors Research Labs, Warren, MI, 1982.

[18] M. Kiskinova, G. Pirug, and H.P. Bonzel, Surf. Sci., 150 (1985), 319.

[19] P.A. Thiel and T.E. Madey, Surf. Sci. Rep., 7 (1987), 211.

[20] (a) S-C. Chang, X. Jiang, J.D. Roth, and M.J. Weaver, J. Phys. Chem., 95 (1991), 5378; (b) X. Jiang and M.J. Weaver, Surf. Sci., 275 (1992), 237.

[21] M.J. Weaver, App. Surf. Sci., 67 (1993), 147.

[22] E. Langenbach, A. Spitzer, and H. Lüth, Surf. Sci., 147 (1984), 179.

[23] For example, D. Eisenberg and W. Kauzmann, "The structure and Properties of Water", Oxford, 1969, Chapter 4.

[24] B.W. Callen, K. Griffiths, and P.R. Norton, Surf. Sci., 261 (1992), L44.

[25] T.H. Ellis, E.J. Kruus, and H. Wang, Surf. Sci., 273 (1992), 73.

[26] Z. Xu, J.T. Yates, Jr., L.C. Wang, and H.J. Kreuzer, J. Chem. Phys., 96 (1992), 1628.

[27] C. Shannon, D.G. Frank, A.T. Hubbard, Ann. Rev. Phys. Chem., 42 (1991), 393.

[28] For example: M.A. Van Hove, R.J. Koestner, J.C. Frost, and G.A. Somorjai, Surf. Sci., 129 (1983), 482.

[29] S-L. Yau, X. Gao, S-C. Chang, B.C. Schardt, and M.J. Weaver, J. Am. Chem. Soc., 113 (1991) 6049.

[30] X. Gao, S-C. Chang, X. Jiang, A. Hamelin, and M.J. Weaver, J. Vac. Sci. Tech., A10 (1992), 2972.

[31] S-L. Yau, Ph.D. thesis, Purdue University, 1990.

[32] I. Oda, J. Innkai, and M. Ito, Chem. Phys. Lett., 203 (1993), 99.

[33] I. Villegas, unpublished results.

[34] C.M. Vitus, S-C. Chang, B.C. Schardt, and M.J. Weaver, J. Phys. Chem., 95 (1991), 7559.

[35] I. Villegas, unpublished results.

[36] I. Villegas, C. Stuhlmann, and M. J. Weaver, to be published.

[37] D.G. Frank, J.Y. Katekaru, D.S. Rosasco, G.N. Salaita, B.C. Schardt, M.P. Soriaga, D.A. Stern, J.L. Stickney, and A.T. Hubbard, Langmuir, 1 (1985), 587.

[38] (a) V.B. Paulissen and C. Korzeniewski, J. Phys. Chem., 96 (1992), 4563; (b) C. Korzeniewski et al, to be published.

[39] T. Wilke, X. Gao, C.G. Takoudis, and M.J. Weaver, J. Catalysis. 130 (1991), 91.

[40] Y. Zhang and M.J. Weaver, Langmuir, 9 (1993), 1397.

[41] Y. Zhang, X. Gao, and M.J. Weaver, J. Phys. Chem., 97 (1993), in press.

[42] For example: P.M. Epperson, J.V. Sweedler, R.B. Bilhorn, G.R. Sims, M.B. Denton, Anal. Chem., 60 (1988), 327A

[43] For a review, see: L.D. Burke and M.E.G. Lyons, in "Modern Aspects of Electrochemistry", Vol. 18, R.E. White, J. O'M. Bockris, and B.E. Conway, eds., Plenum, New York, 1986, Chapter 4.

[44] Y. Zhang and M.J. Weaver, J. Electroanal. Chem., in press.

[45] A. Tolia et al, to be published.

[46] X. Gao and M.J. Weaver, to be published.